

## Rotation of Binary Cyclones—A Data Analysis Study

B. ZIV AND P. ALPERT

*Department of Geophysics and Planetary Sciences, Raymond and Beverly Sackler Faculty of Exact Sciences,  
Tel Aviv University, Tel Aviv, Israel*

(Manuscript received 17 January 1994, in final form 14 September 1994)

### ABSTRACT

In contrast to earlier studies, where only binary tropical storms were explored, the rotation at midlatitude and the subtropics is studied here. The point vortex theory applied to two neighboring cyclonic vortices isolated from external forcing predicts the following features: rotation in a cyclonic sense at a rate directly proportional to the sum of the cyclones' intensities and inversely to the square of their separation, with the weaker cyclone rotating faster than the more intense one. This interaction, noticed in the Tropics, was entitled the Fujiwhara effect or binary interaction. Objective analysis of 17 313 cyclone pairs using ECMWF initialized datasets was done to examine the existence and behavior of binary interaction between extratropical cyclones. The impact of anticyclones is studied through the moments of distribution for the relative vorticity. The anticyclonic shear of the background flow and the prevalence of anticyclones in the subtropics are suggested to explain the absence of binary rotation there. Midlatitude cyclone pairs with separations of up to 2000 km are indeed found to rotate cyclonically about each other at a rate proportional to their combined intensities, in agreement with theory. The binary rotation rate decreases with the square of the separation distance, as in the point vortex theory, up to 1400 km. But a pronounced unexpected peak was found near 1800 km. No significant correlation was found between the individual rotation speeds ratios and that of the intensities of the interacting cyclones. Only partial agreement between the observed rotation of midlatitude surface binary cyclones and the barotropic predictions indicates the need to adopt a more elaborate model. Indeed, the 500-hPa binary interaction study reveals a much better agreement with theory. In a companion study, the authors propose a two-level conceptual model that employs the PV ideas for exploring the binary surface cyclone behavior.

### 1. Introduction

The idea of remote interaction between barotropic vortices was first suggested by Fujiwhara (1923, 1931), employing laboratory experiments. The interaction between two cyclones is expressed in relative cyclonic rotation accompanied by a mutual approaching and was entitled, therefore, the "Fujiwhara effect" (e.g., Brand 1970). It is also called a "binary interaction" (Dong and Neuman 1983) and was quantitatively formulated by Lamb (1945). This effect was found to exist over the tropical oceans, especially in the Pacific. In the words of Haurwitz (1951), "when two tropical cyclones exist simultaneously at the same region" they are called "tropical binary cyclone" or "binary system." The binary interaction is referred to as a source of errors in the forecasting of cyclone tracks (Brand 1970) and was also associated with their "meandering about a longer-term track" (Holland and Lander 1993), which is not well captured by forecast models.

Data analyses have attempted to study the behavior of tropical binary systems to obtain the quantitative features of the Fujiwhara effect and its dependence on the parameters of the binary systems. A major difference was found between tropical cyclone pairs in the Pacific and those in the Atlantic. The Pacific binary systems indeed rotate cyclonically, whereas those in the Atlantic rotate, in general, anticyclonically (Hoover 1961; Dong and Neuman 1983). This difference was attributed to the corresponding large-scale background flow and its impact on the interacting cyclones. Consequently, most of the analysis was performed with Pacific data.

Haurwitz (1951) developed a method for computation of the rotation rate of binary cyclones from the structures of the individual cyclones. The results showed qualitative agreement with observations for eight cases where data was relatively reliable. He attributed the observed deviations from theory to the paucity of observations, the deviation of the vortices' structure from the idealized model, and the influence of the steering currents. Brand (1970) used 22 cases for the period 1953–67 containing 266 time sets over the Pacific with a typhoon intensity. He found an effective interaction radius of about 750 n mi (1400 km) and obtained a quadratic functional dependence of rotation

*Corresponding author address:* Dr. Pinhas Alpert, Department of Geophysics and Planetary Sciences, Tel Aviv University, University Campus, Ramat Aviv, 69978 Tel Aviv, Israel.

rate with distance, in good agreement with theory. Dong and Neuman (1983) studied extensively the rotation of binary tropical cyclones both in the Atlantic and in the Pacific. They studied the contribution to the rotation due to the steering by the sheared background flow and found it comparable with that of the binary interaction, although smaller. They also divided the binary systems into two categories according to their intensities and found that when the separation distance is less than 650 km, the intense systems rotate significantly faster.

Numerical simulations of tropical binary cyclones were performed using a barotropic and a nondivergent model (Chang 1983; DeMaria and Chan 1984) and showed high sensitivity of the cyclones' tracks to their assumed flow structures. Three-dimensional simulations, including both friction and diabatic heating, showed very good agreement with the theory (Chang 1983). Falkovich et al. (1995) examined the role of both the beta effect and the ocean feedback upon tropical binary storms. They found the beta effect to be a source of asymmetry in the development of the individual cyclones' intensities and, hence, in their tracks, whereas the ocean feedback has a dissipating effect for both this asymmetry and the system intensity as a whole.

Haurwitz (1951) stated that "it seems unlikely that the theory in its simple form can be applied generally to extratropical cyclones and anticyclones because the deviations from barotropic stratification are presumably large, so conditions aloft are quite different from those near the surfaces." The motivation for this work is the question whether the binary interactions are a significant phenomenon in the extratropics, particularly over the midlatitude zone, concentrating on their rotational relative motion as exemplified in Fig. 1. The analysis is based on cyclone locations and tracks (Alpert et al. 1990a,b) extracted objectively from ECMWF initialized data. Contrary to the tropical binary cyclones' analyses, which excluded cases where the cyclones did not attain a "storm" intensity, the present analysis includes all cyclones detected within the study domain and period. Selections are done only for cases in which the background is "noisy," for example, when any additional cyclone is found in the close vicinity of a binary system or when a system is located in a cyclogenetic region. Section 2 below presents a case study, which demonstrates the hypothetical cyclones' relative motion. Section 3 presents the features of the binary rotation according to the point vortex theory. In section 4, we describe the method used to analyze the cyclones' relative rotation, while in section 5 the impact of anticyclones upon binary systems is estimated. Section 6 deals with the external forcing affecting binary cyclones and the method used to reduce their impact upon the studied sample. In section 7 the results for midlatitude binary cyclones are presented. Section 8 compares the predicted rotation rates ex-

pected for mid- and lower-latitude binary systems with the observations. In section 9, the role of the background shear upon the binary systems is estimated and discussed. Sections 10 and 11 summarize the results and outline further research. In appendix C, results for the 500-hPa binary interactions are shown, and compared to surface characteristics.

## 2. Case study: 22–23 Dec 1986

The motion of two cyclones during 22–23 Dec 1986 over Europe demonstrates the cyclonic rotation of two neighboring cyclones. Figure 1 shows a time series of the 1000-hPa geopotential height charts using the processing system developed by Neeman and Alpert (1990). On 0000 UTC 22 Dec 1986 two cyclones marked A and B are located at Latvia (57°N, 27°E) and northern Italy (42°N, 12°E). The northern cyclone moves west, while the southern one moves to the east-southeast. The relative motion of a cyclone pair can be visualized by tracing the temporal change in the orientation of their connection line. It rotates cyclonically from 40° to 320° (i.e., 80° within 36 h).

## 3. Theoretical considerations

Theories considering two-dimensional inviscid flow, conserving absolute vorticity (Lamb 1945; Batchelor 1980; Aref 1983) as well as laboratory experiments (Fujiwhara 1931; Hopfinger and Van Heijst 1993) have been extensively used to study the interactive behavior of vortices. A common theory is the point vortex theory. The latter replaces each vortex with a "point" having an infinitely small core with infinitely high vorticity represented by a  $\delta$  function embedded in a flow having zero vorticity. A single number, positive for a cyclonic vortex and negative for an anticyclonic one, characterizes its intensity. As a material tracer, each point vortex is subjected to the superposition of circular flow patterns induced by the other vortices. For a point vortex  $i$  the motion due to the presence of the other point vortices  $j$  is given by (Batchelor 1980)

$$\begin{aligned} \frac{dx_i}{dt} &= -\frac{1}{2\pi} \sum_{j=1, j \neq i}^N \frac{k_j (y_i - y_j)}{r_{ij}^2}; \\ \frac{dy_i}{dt} &= \frac{1}{2\pi} \sum_{j=1, j \neq i}^N \frac{k_j (x_i - x_j)}{r_{ij}^2}, \end{aligned} \quad (1)$$

where  $x_i$ ,  $y_i$  and  $x_j$ ,  $y_j$  are the horizontal coordinates, and  $k_i$ ,  $k_j$  are the intensities of the point vortices  $i$  and  $j$ , respectively. The separation distance  $r_{ij}$  is given by  $[(x_i - x_j)^2 + (y_i - y_j)^2]^{1/2}$ . The intensity has dimensions of meters squared per second, indicating that it is the integral of the vorticity over the small but finite core area of the vortex, which is equal to the circulation along a curve that encircles it. Integration of (1) for a finite number of vortices is obtainable. The model can

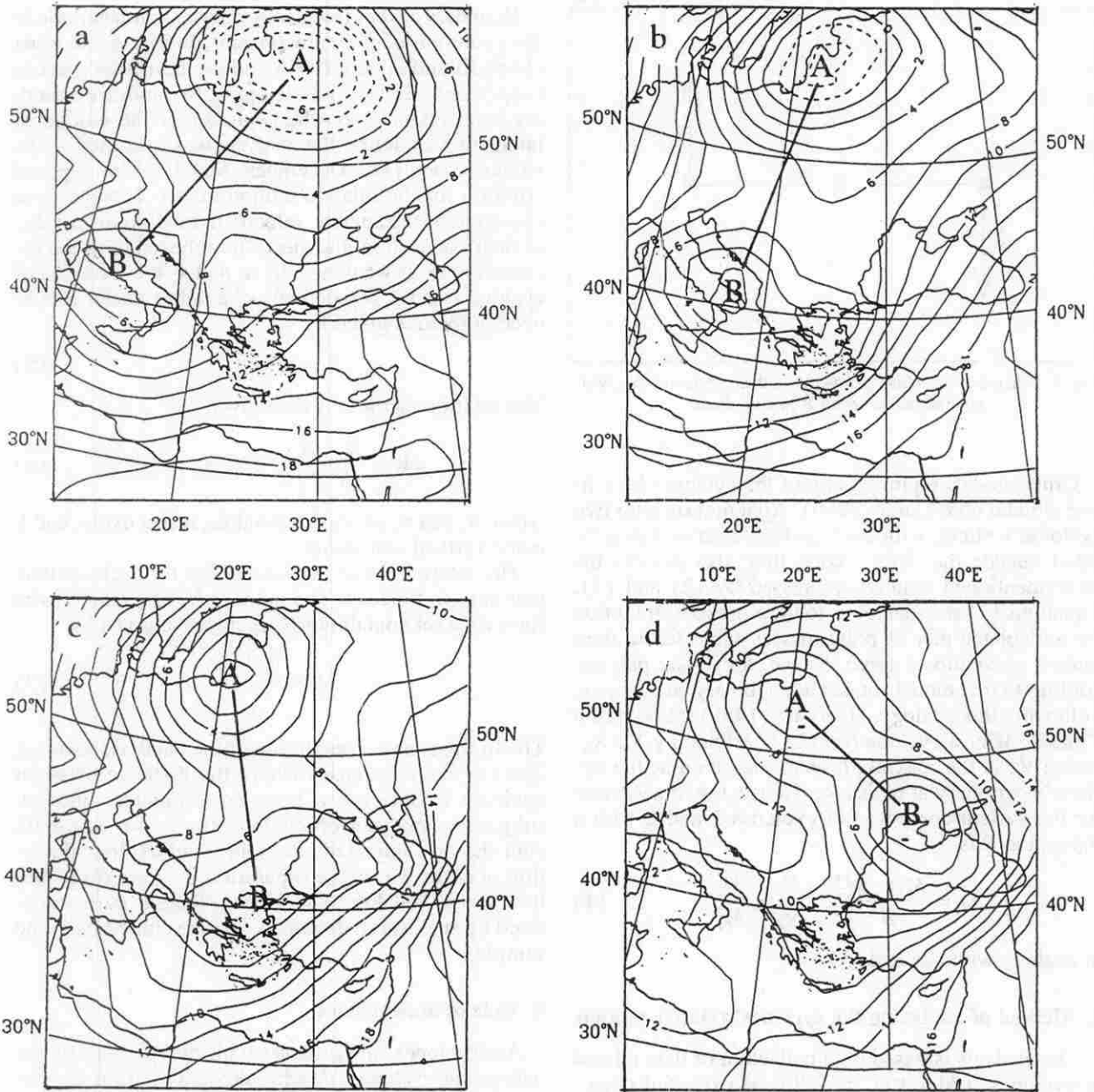


FIG. 1. The 1000-hPa geopotential height distribution in dekameters with a 2-dm interval for: (a) 0000 UTC 22 December 1986, (b) 1200 UTC 22 December 1986, (c) 0000 UTC 23 December 1986, and (d) 1200 UTC 23 December 1986. Cyclone centers composing the cyclone pair are denoted by A and B. Dashed lines represent negative values.

be applied to rotating frames (Hopfinger and van Heijst 1993), where the dynamic fields are measured relative to the reference frame.

When (1) is applied to two cyclonic point vortices ( $k_1, k_2 > 0$ ) with a separation distance  $R$ , their mutual rotation has the following features. They move cyclonically about a point, which is located on their connecting line, and their rotation rate  $\omega$  is proportional to their combined intensities but inversely to their separation according to (Batchelor 1980),

$$\omega = \frac{k_1 + k_2}{2\pi R^2}. \quad (2)$$

In addition, their motion is perpendicular to the connection line and their individual speeds obey the ratio

$$\frac{V_1}{V_2} = \frac{k_2}{k_1}, \quad (3)$$

where  $V_1$  and  $V_2$  denote the speeds of cyclone 1 and 2, respectively (Fig. 2).

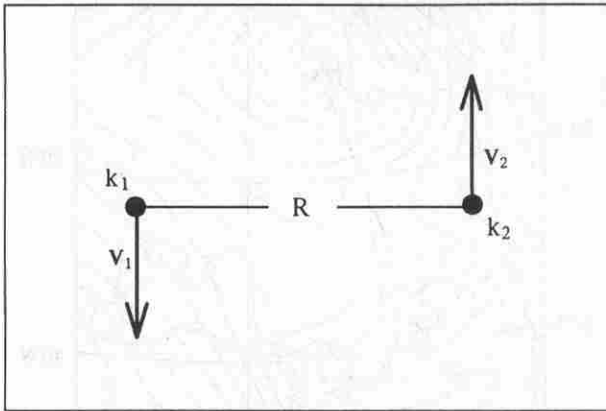


FIG. 2. Scheme of a cyclone pair ( $k_1, k_2$ ), their velocities ( $V_1, V_2$ ), and the radius vector  $R$  joining them.

Other models represent any of the cyclones by a finite circular core (James 1950). Applying such for two cyclonic vortices, with each cyclone's center being located outside the other's core, they also possess the abovementioned features expressed by (2) and (3). Equations (1) are analogous to the equations of motion for an isolated pair of point masses subjected to their mutual gravitational force. Hence, a cyclone pair according to this model rotates like a binary star system. Following this analogy, Haurwitz (1951) introduced a "mass"  $M$  of a cyclone ( $=k/2\pi$ ), defined by  $V_m \cdot R_m$ , where  $V_m$  is the maximum wind measured at the cyclone's periphery at radius  $R_m$ . Hence, the rotation rate for the system composed of cyclones 1 and 2 with a separation  $R$  is

$$\omega = \frac{M_1 + M_2}{R^2}; \quad \frac{V_1}{V_2} = \frac{M_2}{M_1}, \quad (4)$$

in analogy with (2) and (3).

#### 4. Method of analyzing the cyclones' relative motion

The analysis is based on a collection of data related to cyclones<sup>1</sup> (Alpert et al. 1990a,b) extracted objectively from 1000-hPa geopotential fields of the ECMWF initialized datasets (Bengtsson et al. 1982; Haseler and Sakellarides 1986; and Hollingworth et al. 1986) containing atmospheric variables in the 0°–60°N, 0°–60°E domain for the years 1982–88. This collection is partitioned into 1440 time sets with a 12-h interval containing their locations, minimum height, and the Laplacian of the geopotential field at their centers. The velocity of a cyclone for a certain time was defined according to its track increment done within the following 12-h time interval.

<sup>1</sup> A "cyclone" is defined at the location of a minimum in the 1000-hPa geopotential height over a 500 × 500 km<sup>2</sup> (Alpert et al. 1990a).

Boundary-layer effects may play a significant role in the evolution of pressure systems during the summer (Shay-El and Alpert 1991) and the transition seasons (Alpert and Ziv 1989). Attempting to minimize boundary layer effects upon the evolution or the motion of interacting cyclones, the analysis was restricted to the winter season (i.e., December–March). The required criterion for the relative motion of two cyclones was chosen to be the angular velocity in revolutions per day of their connection line, hereafter referred to as the rotation factor. If we denote by  $x_1$  and  $x_2$  the locations of cyclone 1 and 2, respectively, the radius vector  $R$  connecting them is given by

$$R = x_2 - x_1. \quad (5)$$

The rotation factor  $\omega$  is then given by

$$\omega \mathbf{k} = \frac{R \times \dot{R}}{R \cdot R}; \quad \dot{R} = v_2 - v_1, \quad (6)$$

where  $v_1$  and  $v_2$  are their velocities, respectively, and  $\mathbf{k}$  is the vertical unit vector.

The rotation factor was computed for each cyclone pair at each time set. The number  $N_p$  of cyclone pairs for a time set containing  $N_c$  cyclones is given by

$$N_p = \sum_{i=1}^{N_c-1} i. \quad (7)$$

The limited spatial resolution of the database to about 250 km excludes cases where the distance between cyclones is only a few hundred kilometers. Indeed, subjective analysis of cyclone tracks for 1 month (not shown) indicated unreliability of cyclone detection in cases where the separation distance drops below about 500 km. Therefore, cyclone pairs separated by such small distances were excluded from the sample.

#### 5. Role of anticyclones

Anticyclones may interact with one or both of the interacting cyclones, causing deviations from the expected routes. Anticyclones' intensity are expected to be weaker than cyclones because when gradient balance exists, "the pressure field near the center of a high is always flat and the wind gentle compared to the region near the center of a low" (Holton 1992). To verify this hypothesis, we made a comparative study of the first three moments of the 1000-hPa relative vorticity field. The  $i$  moment  $M_i$  of a variable  $f$  over a domain  $A$  is given by

$$M_i = \left( \frac{1}{A} \int_A f^i dA \right)^{1/i}, \quad (8)$$

where  $dA$  is a surface element.

The first moment, that is,  $i = 1$ , yields the average of the  $f$  field, while the second is the standard deviation,



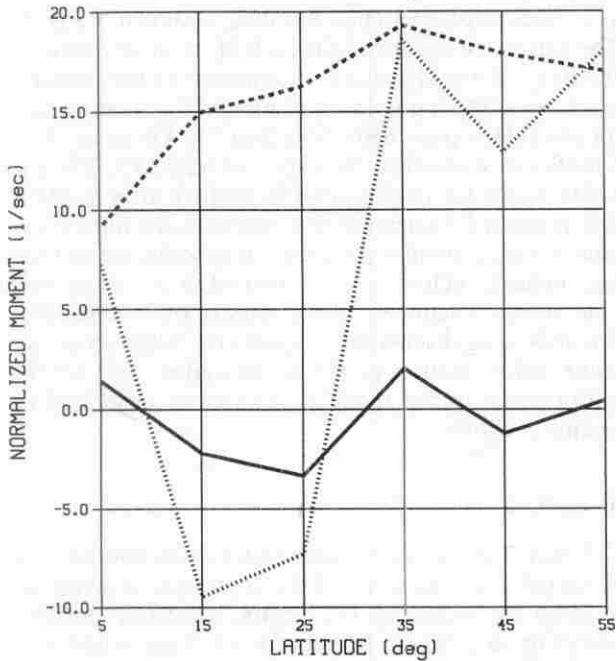


FIG. 3. Latitudinal variation of the first (solid), second (dashed), and third (dotted) moments of relative vorticity in units of  $10^{-6} \text{ s}^{-1}$  averaged for 315 time sets from the period 1982–88 for the months December–March.

and the third reflects the degree of asymmetry between the positive and the negative field's anomalies. Figure 3 presents the latitudinal variation of the three moments averaged over 315 sets chosen at random out of the study period. The study domain was divided into six latitudinal belts, each including 125 grid points. The first moment (i.e., the average) indicates that the average relative vorticity undulates about zero, except for the subtropical latitudes  $15^{\circ}$ – $25^{\circ}\text{N}$ , where it is negative and attains the value of  $-3 \times 10^{-6} \text{ s}^{-1}$ , probably reflecting the dominance of the subtropical highs. The third moment shows substantial differences among the latitudinal belts. At midlatitudes its value is positive and rather high compared to the first moment, indicating a structural difference between the cyclones and anticyclones and meaning that even though the cyclones cover a smaller area, their amplitude significantly exceeds that of the anticyclones. The third moment is negative, with a relatively small absolute value between  $25^{\circ}$  and  $15^{\circ}\text{N}$ . This suggests that the above hypothesis holds only for the midlatitudes from  $30^{\circ}\text{N}$  poleward. In terms of point vortices, one may approximate the surface flow at midlatitudes by finite-positive strong point vortices surrounded by a "cloud" of weak negative point vortices. This supports the ignoring of the midlatitude anticyclones' role upon interacting cyclones but not at lower latitudes. Our discussion will, therefore, concentrate on the midlatitudes cyclones, bearing in mind that in some cases the binary

interaction may be disturbed by interaction with anticyclones.

## 6. Reduction of external forcing

In real cases binary cyclones may be subjected to the influence of "external" forcing. To get closer to the net mutual effect, the analysis was redone, after removal of the noisy cases.

### a. Coexistence of additional cyclones

Cyclone pairs around which no other cyclone was found over some distance  $r$  are referred to as "isolated pairs." Since a selection of isolated pairs with the use of a relatively large  $r$  considerably reduces the sample's population,  $r$  was chosen to be 1000 km, implying that even an isolated pair may be subjected to some interaction with remote cyclones.

### b. Geographic effects

Approaching certain areas, a cyclone may be deflected from its expected path of an idealized point vortex. Such, for instance, may be cyclogenetic areas. Figure 4 shows the spatial distribution of cyclone occurrences for the studied period. It indicates, in accordance with Alpert et al. (1990a), the existence of small and significant cyclogenetic sites located at the southern Caspian Sea, along the Mediterranean and at the eastern Black Sea, covering a small portion of the entire domain. These areas are mainly over water bodies or at the lee of mountain ridges. As suggested by many investigators (e.g., Mattocks and Bleck 1986; Tafferner 1990; Stein and Alpert 1993), the lee cyclogenesis is a manifestation of a mountain ridge's blocking effect on air masses and their properties. Such areas are, therefore, supposed to attract approaching cyclones and

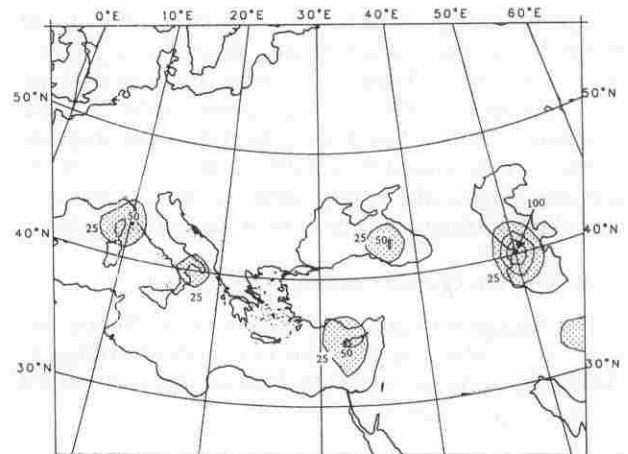


FIG. 4. Cyclone occurrences for the same period as in Fig. 3 at  $2.5^{\circ} \times 2.5^{\circ}$  with an interval of 25. Areas with values exceeding 25 are shaded.

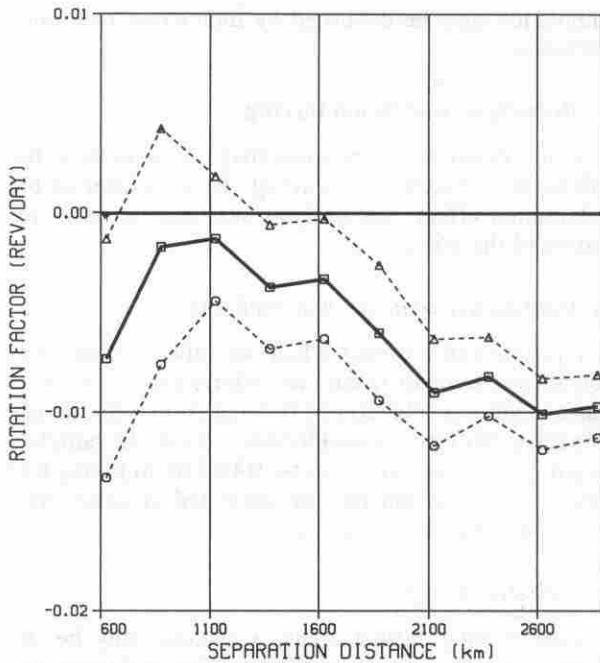


FIG. 5. Variation of the average cyclones' pairs rotation factor in units of rotations per day as a function of their separation distance (solid) for the area ( $0^{\circ}$ – $60^{\circ}$ N,  $0^{\circ}$ – $60^{\circ}$ E) for the same period as in Fig. 3. Each point represents average value for a 250-km interval. Dashed lines indicate the limits of 98% confidence interval, given by:  $(\text{STD} \times 2.326)/N^{1/2}$ , where STD is the rotation factor's standard deviation and  $N$  is the sample size.

also to hinder their motion. To avoid cases where these effects upon moving cyclones may be significant, the analysis was redone, but with the exclusion of cases where any of the interacting cyclones was found in a cyclogenetic region (shaded regions in Fig. 4). The remaining pairs will be named as "free pairs."

*c. Westerly drift*

Midlatitude cyclones tend to migrate eastward due to the basic-state westerlies and their steering effect (e.g., Gill 1982). Here, we assume that the cyclone pairs' relative rotation is superposed upon a zonal translation. Rather than dealing with the individual velocities, we measured the rotation rates of the connection line joining the binary members and so circumvented the translation impact upon the binary systems.

*d. Role of background shear*

The background flow may have a shear. Hence, besides its translational effect, it may also contribute to the rotation of binary systems. This subject is discussed separately in section 9.

**7. Observed features of binary cyclones**

The average rotation factor for the entire area and all the detected cyclones, including 17 313 cyclone pairs,

as a function of separation distance, is shown in Fig. 5. The values are negative (anticyclonic relative rotation) for most of the distances, in contrast to the model's prediction. The latitudinal variation of the rotation factor of cyclone pairs being less than 750 km apart (Fig. 6) reflects, somewhat, the expected tendency. The rotation factor for midlatitudes is positive from  $\sim 30^{\circ}$ N and poleward, indicating that midlatitudes binary cyclones with a small separation (in synoptic terms) rotate, indeed, cyclonically, in contrast to the lower-latitude binary cyclones, where anticyclones dominate. The following discussion considers the behavior of cyclone pairs' motion at the midlatitudes ( $30^{\circ}$ – $60^{\circ}$ N) with respect to the model's features as described in section 3 above.

*a. Cyclonic rotation*

Figure 7 shows the rotation factor of midlatitude cyclone pairs as a function of the separation distance up to 2900 km including 1423 pairs, indicating positive values up to 2100 km (except for 1375 km, where it is zero). The positive values, corresponding to the expected cyclonic relative motion, have 98% statistical reliability up to 1100 km. The percentage of cyclone pairs separated by 2000 km or less rotating cyclonically is 59%. To reduce external effects, the sample was reduced to pairs around which no other cyclones were found within 1000 km and where none of the cyclones were located at a cyclogenetic area (i.e., isolated and

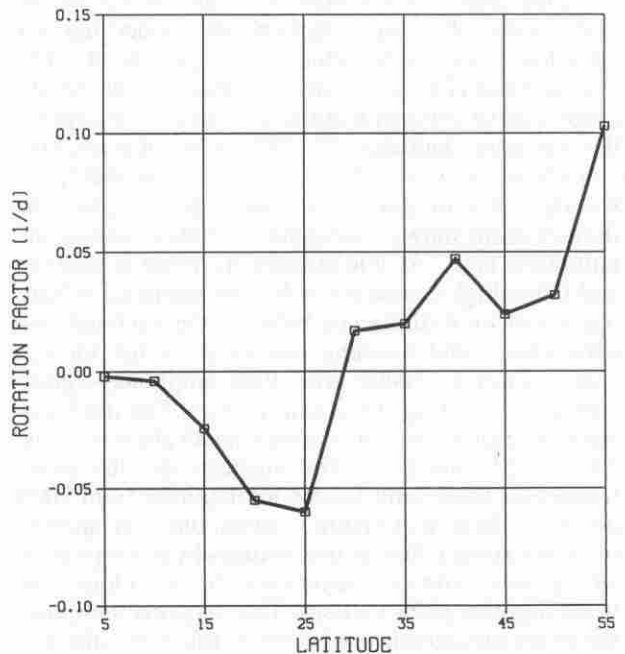


FIG. 6. Average rotation factor of cyclone pairs separated by 500–750 km for the same period as in Fig. 3 for latitudes  $5^{\circ}$ – $55^{\circ}$ N. Each value is the average over a latitudinal band of  $10^{\circ}$ .

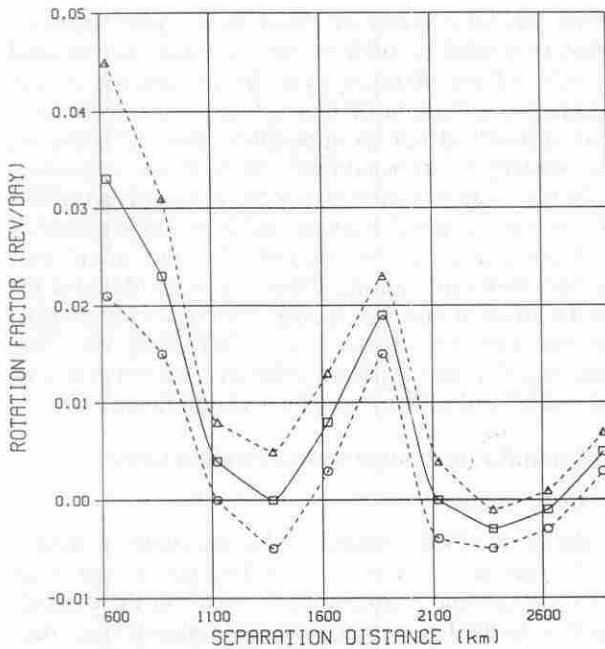


FIG. 7. As in Fig. 5 but for the latitudes  $30^{\circ}$ – $60^{\circ}$ N. Containing 1423 cyclone pairs.

free pairs). In the reduced sample it became 72%. The respective values are 28% for the Atlantic (Brand 1970) and 70% for the Pacific tropical storms (Dong and Neuman 1983). Cyclone pairs separated by more than 2000 km were found to rotate cyclonically in about 50% of the cases even for the reduced sample, indicating insignificant binary interaction.

Hereafter, the cyclonically rotating midlatitude cyclone pairs with separation less than 2000 km will be referred to as "midlatitude binary cyclones."

#### b. Rotation and cyclones' separation

The model, that is, (2), predicts an inverse dependence of the rotation factor on  $R^2$  (see the semidashed curve in Fig. 8). In this figure, an agreement is found with the theoretical relation for distances smaller than 1400 km, but between 1600 and 2000 km a pronounced peak is found. Figure 8, dashed, indicates no significant change of rotation factor for isolated pairs at all distances. For isolated and free pairs, the rotation values (Fig. 8, dotted) are significantly increased. To confirm the statistical basis for the above results, the sample was arbitrarily divided into two independent subsamples, for the years 1982–85 and for 1986–88. The functional dependence of the rotation factor on separation was then compared for the full subsamples and for the reduced isolated and free version. The results were similar in their functional dependence, except for a difference in the average values. In one of the subsamples, however, the average rotation factor for all the pairs

was slightly negative ( $-0.0001$  to  $-0.0064$  day $^{-1}$ ) for the distance range of 1000–1750 km. But, for the "clean" (i.e., isolated and free) pairs, the corresponding values for the same range became positive (0.01 to 0.029). The following discussion focuses on the 327 clean pairs.

#### c. Rotation and cyclones' intensities

The model predicts linear dependence of the rotation factor of a binary cyclone on their combined intensities, that is, (2). The intensity of a vortex is the integrated relative vorticity over its core area. Hence, it is expected to be proportional to the relative vorticity at its center. This was approximated by the geostrophic component  $\zeta_g$ , which may be extracted from the Laplacian of the geopotential height  $h$  according to

$$\zeta_g = \mathbf{k} \cdot (\nabla \times \mathbf{V}_g) = \frac{g}{f} \nabla^2 h, \quad (9)$$

where  $g$  is gravity and  $f$  is the Coriolis parameter. Figure 9a shows the variation of the average rotation factor with the mean geostrophic relative vorticity of the binary cyclones with separation of 500–2250 km. Indeed, the rotation factor increases with relative vorticity but not monotonically. The relative vorticity at the cy-

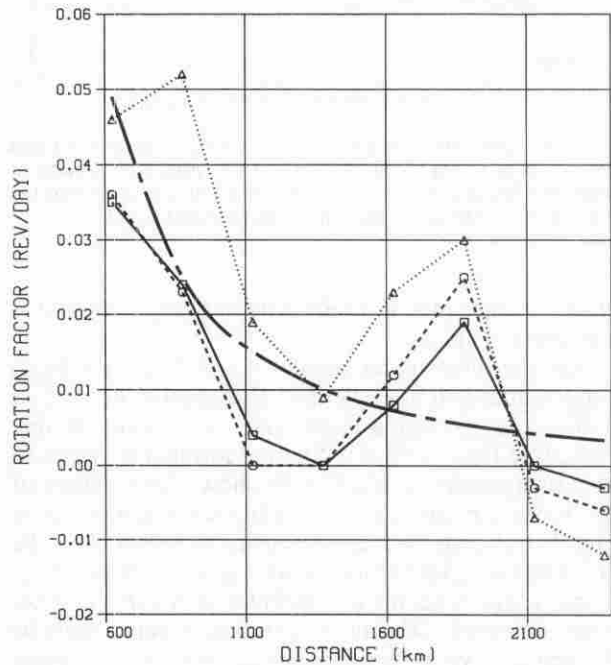


FIG. 8. Average rotation factor for the area and period as in Fig. 7 (solid), for cyclone pairs around which no other cyclone was detected within a radius of 1000 km, that is, isolated pairs, containing 628 pairs (dashed) and for isolated free pairs excluding cases where any of the cyclones was located in a cyclogenetic area containing 327 pairs (dotted). The semidashed line shows the theoretical relationship.

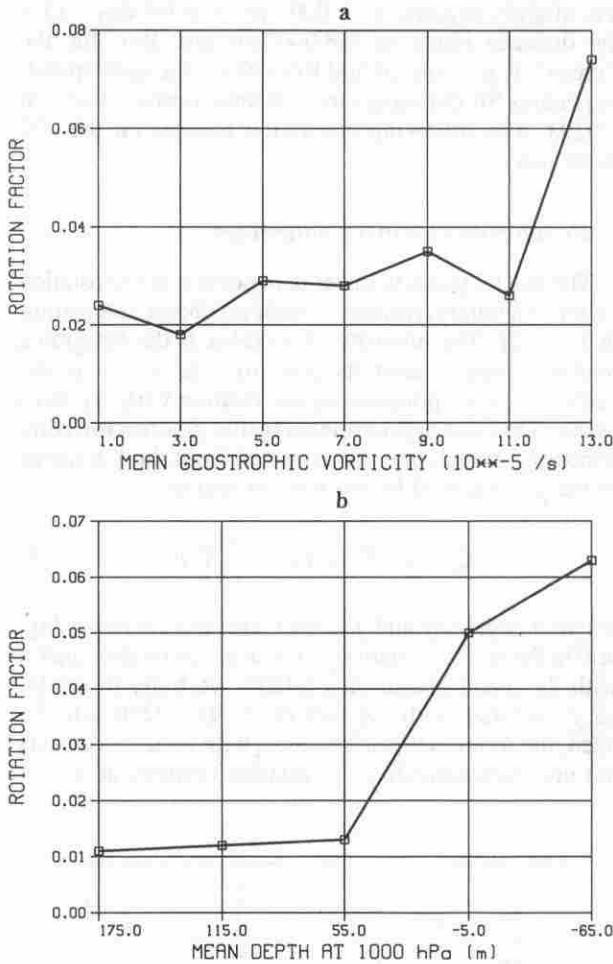


FIG. 9. Variation of rotation factor with the mean intensity for area and period as in Fig. 7 for isolated and free pairs with a range of separation distances 500–2250 km. The intensity is expressed by (a) vorticity of geostrophic wind and (b) geopotential height.

clone's center may not reflect its intensity, unless it is weighted by its core size.

Another intensity parameter of a cyclone may be its geopotential height depletion. The relation between a midlatitude cyclone's depth and its intensity is discussed by James (1950). Another formula is proposed here in appendix A, and Fig. 9b shows the variation of the average rotation factor for the same sample as in Fig. 9a but with the mean intensity as reflected by the geopotential height of the cyclone pairs' centers, (A4). It seems that here, the agreement with theory is somewhat improved. Of course, a cyclone's depth must be defined relative to its surroundings, but on the average it may serve as a better indicator for the intensity.

*d. Relation between the cyclones' individual intensities and rotational speed*

This relation may be examined by the correlation between  $V_1/V_2$  and  $k_2/k_1$  of the binary cyclones. To

avoid the false effect of zonal background steering, there is a need to subtract the common translational velocity of the binary system. In the absence of any acceptable definition of this velocity, this becomes a very difficult, if not an impossible, task. If, however, this velocity is extracted from the cyclones' individual velocities, unproductive results are obtained (appendix B). Assuming zonal background flow, the correlation was computed accounting only for the meridional speeds. Poor correlations, about 0.1, were obtained for all the isolated and free binary cyclones with positive rotation rates for separations of 500–2000 km. This indicates that the expected relation between ratios of intensities and rotation speeds is insignificant.

**8. Quantitative evaluations of rotation rates**

*a. Case studies*

Haurwitz (1951) referred to binary cyclones, where each cyclone is located outside the other's core, with zero background vorticity (Fig. 10). He then developed a method for computing the rotation rate from their masses, which sums up to (4). Here, each mass was determined assuming a gradient balance and using the gradient of the geopotential height at the 1000-hPa cyclone's periphery. The 24-h rotation for two case studies was computed. The first case is shown in Fig. 1 and the other is a binary cyclone that prevailed for 36 h during 3–5 January 1985 over eastern Europe (not shown). The computed results were  $17^\circ$  and  $16^\circ$ , while the observed values were  $60^\circ$  and  $65^\circ$ , respectively, about three times larger than the predicted values. A possible reason for this discrepancy is the role of the upper-level cyclones (Ziv and Alpert 1994).

*b. Rough estimations—the patch vortex model*

The idea of isolated cyclonic vortices embedded within an anticyclonic background cloud (section 5)

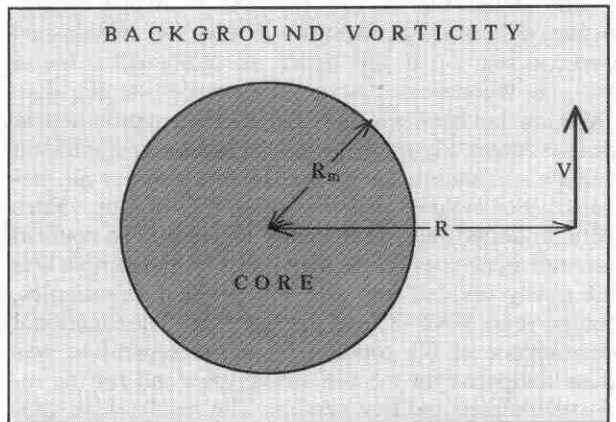


FIG. 10. Scheme of a cyclone with a finite core (heavy shading) of radius  $R_m$  and induced tangential velocity  $V$  at radius  $R$  from its center embedded in a background uniform vorticity (light shading).



may be expressed by the following simple model for the rotation factor. Consider two identical cyclones, each with a core of radius  $R_m$  with uniform relative vorticity  $\zeta_0$  (Rankine vortex). They are embedded in a medium with a uniform negative background vorticity  $\zeta_b$  (Fig. 10) and separated by  $R$ , while  $R > R_m$ . The circulation  $C$  over a circular curve with radius  $R > R_m$  encircling one of the cyclones is

$$C = \int_{\text{core}} \zeta_0 ds + \int_{\text{out of core}} \zeta_b ds \\ = \pi[\zeta_0 R_m^2 + \zeta_b(R^2 - R_m^2)], \quad (10)$$

where  $ds$  is an area element. For a point vortex or when  $\zeta_b = 0$ , the circulation is identical to the intensity. The rotational speed  $V$  induced by this cyclone at distance  $R$  is, therefore,

$$V = \frac{[\zeta_0 R_m^2 + \zeta_b(R^2 - R_m^2)]}{2R}. \quad (11)$$

From (2) and (11) the rotation factor  $\omega$  due to the contributions of both cyclones is

$$\omega = \left(\frac{R_m}{R}\right)^2 (\zeta_0 - \zeta_b) + \zeta_b. \quad (12)$$

For  $R \gg R_m$  the rotation factor approaches  $\zeta_b$ . Assuming  $|\zeta_0| \gg |\zeta_b|$ , one may expect cyclonic rotations for small separation and a reversal in the sense of rotation at a critical radius  $R_c$ , where

$$R_c = R_m \left( \frac{\zeta_b - \zeta_0}{\zeta_b} \right)^{1/2}. \quad (13)$$

Equations (12) and (13) imply that the rotation rate and the critical radius are highly sensitive to the choice of the background vorticity.

Here, the typical critical radii and rotation rates for different latitudinal belts are evaluated, employing approximated values for  $R_m$ ,  $\zeta_0$ , and  $\zeta_b$ . The choice of characteristic vorticities for evaluation of the typical rotation rates of cyclone pairs with  $R_m = 250$  km and for several latitudinal belts was based on the sample used to study the 1000-hPa vorticity field (section 5). As the background vorticity we applied the mode value at the respective latitudinal belt. The mode of the geostrophic vorticity at the centers of the midlatitude cyclones may overestimate the real vorticity there and particularly over the finite core. An alternative may be the rms of the positive vorticities over the respective area. Since the respective values for the two choices at 30°–60°N were found to be  $6 \times 10^{-5} \text{ s}^{-1}$  and  $1.8 \times 10^{-5} \text{ s}^{-1}$ , respectively,  $\zeta_0$  was estimated by  $4 \times 10^{-5} \text{ s}^{-1}$ . For the 10°–30°N the rms was  $1.3 \times 10^{-5} \text{ s}^{-1}$ , hence, the chosen value for the cores' vorticity was  $3 \times 10^{-5} \text{ s}^{-1}$ . The background value was  $1 \times 10^{-6}$  for both middle and lower latitudes.

Equation (13) then yields critical radii of 1600 and 1400 km for the mid- and the lower-latitude binary cyclones, respectively. These values correspond to the minimum in the rotation rates obtained at the midlatitudes near a 1400-km separation. Not so with the negative rotation rates of subtropical latitude cyclone pairs that were found at small separations. The calculated rotation rate for the midlatitude binary cyclones with 600-km separation is  $0.083 \text{ day}^{-1}$ , about twice that observed. The rotation factor for a 1000-km separation is  $0.021 \text{ day}^{-1}$ , which is quite close to the observed value. This model does not explain, however, the peak found near the 1800-km separation. This may be explained, for instance, by core sizes and vorticity values being larger than those assumed here, as can be seen in Fig. 1. This matter is beyond the scope of the present study.

## 9. Contribution of the background shear

Binary rotation rates are determined by the Fujiwhara effect but may be strongly influenced by the shear of the background flow. Dong and Neuman (1983) deduced the orientation of the background shear from the directional variation of the rotation rates of several binary tropical cyclones. Since the flow is assumed nearly zonal over most of the medium and upper troposphere, we specified the background conditions according to the average field of the zonal wind  $\bar{u}$  at the study domain and period. The respective meridional average shear was examined (not shown) and found to be one order of magnitude smaller than the zonal, and, hence, its contribution is ignored. The vertical cross section for  $\bar{u}$  averaged over 0°–60°E longitudes through 0°–60°E latitudes for the study period is shown in Fig. 11. It indicates an average cyclonic shear from ~28°N poleward and anticyclonic shear at the lower latitudes. Gill (1982) refers to the 600 hPa as the steering level for midlatitude systems (horizontal line in Fig. 11). Adopting the average zonal wind as the background flow yields a small cyclonic background steering shear of about  $1.6 \times 10^{-6} \text{ s}^{-1}$  at the 30°–60°N latitudinal belt, which is significantly smaller than the actual rotation of binary systems there. In addition, a considerable anticyclonic shear of about  $-9 \times 10^{-6}$  is found at the 5°–25°N latitudinal belt, comparable to the rotation rates there. Dong and Neuman (1983), attempting to quantify the contribution of the background shear to the rotation of binary cyclones, subtracted the rotation rates of binary systems oriented parallel from those oriented perpendicular to the background shear. Besides reducing the sample size, that approach has a bias due to the variation in the direction of the binary rotation induced by the beta effect (Falkovich et al. 1995).

We have quantified the zonal shear effect by subtracting the rotation rates obtained using their zonal cyclone speeds from that obtained accounting only for their meridional speeds for all the isolated and free bi-

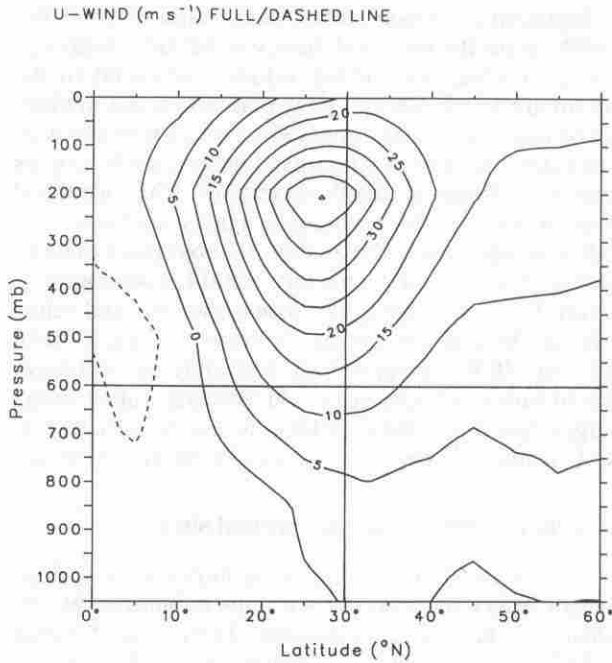


FIG. 11. Vertical cross section of the average zonal wind speed over the 0°–60°E longitudinal band for December–March (1982–1988) in meters per second with a 5 m s<sup>-1</sup> interval. The dashed contour encircles values below -5 m s<sup>-1</sup>.

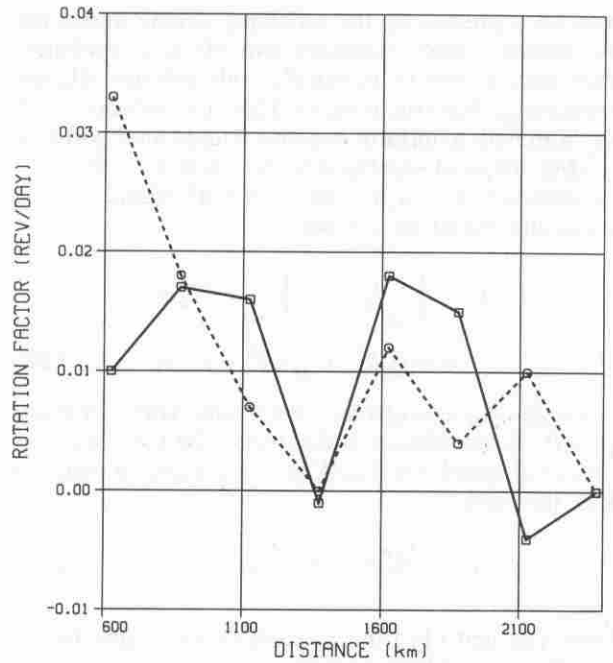


FIG. 12. Variation of rotation factor with separation distance for isolated and free pairs over the 30°–60°N latitudinal belt accounting only for the meridional rotational component (solid) and only for the zonal rotational component (dashed).

nary systems. Figures 12 and 13 show the results as a function of separation for the domain 30°–60°N and 0°–30°N, respectively. From Fig. 12 it seems that at separations smaller than 900 km the background steering indeed contributes significantly, since values there are larger than for pure interaction, assumed to be represented by the meridional component (double at 600 km), but no consistent effect is noticed at larger separations. At lower latitudes, however (Fig. 13), the negative steering effect is much larger than that of the pure interaction, which is also found to be slightly anticyclonic (bold).

10. Discussion

Most cyclone studies, particularly at extratropical latitudes, consider the cyclones as a part of tropospheric disturbances and treat them through wave theories (e.g., Gill 1982; Holton 1992). They consider the interaction between the disturbances and the basic state having a zonal character. The present study concentrates on the mutual interaction among these disturbances.

Objective tracking of 1423 cyclone pairs in the 30°–60°N domain confirms the existence of midlatitude binary cyclones. The binary interactions are effective within the separation of 2000 km. As expected, 2000 km is comparable with the Rossby radius of deformation for midlatitudes. The rotation rates of these binary

cyclones are in agreement with theoretical computations and are of the order of  $5 \times 10^{-2} \text{ s}^{-1} \text{ rev day}^{-1}$ . The increase in the average rotation rate for the reduced

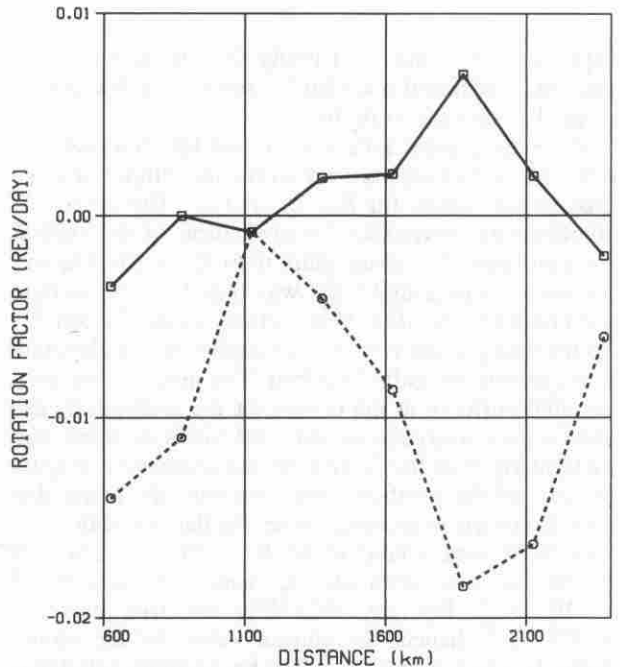


FIG. 13. As in Fig. 12 but for the 0°–30°N latitudinal belt.

sample, after removal of factors that represent external forcing, support the binary interaction as an inherent characteristic of midlatitude cyclones. This is further supported by the increase in the percentage of cyclone pairs rotating cyclonically from 59% to 72% in the reduced sample.

The cyclonic shear of the background midlatitude flow has a significant impact on the rotation of the binary systems with separations less than 900 km. At distances larger than 2000 km the rotation rates undulate around zero, suggesting a cancellation between the slightly negative background vorticity at the surface and the positive background midtropospheric shear.

Deviation of the observed features from the barotropic theory (Table 1) may result from various factors. However, some findings, like the relatively high rotation rates of binary cyclones with separation of about 1800 km and the weak speed/intensity relation, indicate that the interaction between the cyclones is more complex than the two-dimensional model can describe. One source for the disagreement between results and theory may be the model's underlying conception of the surface cyclone as an atmospheric tracer. This is not valid, in general, neither for a pressure minimum nor for a relative vorticity maximum. A parallel study for 500-hPa vortices shows a much better agreement with the above theory (appendix C).

## 11. Summary

Objective tracking of 17 313 cyclone pairs in the 0°–60°N domain gives the following results:

- 1) There is a significant binary interaction at midlatitudes but definitely not at the subtropics.
- 2) The lack of binary interaction at the subtropics is attributed to both the upper-level anticyclonic shear and to the prevalence of surface anticyclones there. The latter is demonstrated by the third moment of the relative vorticity.
- 3) At midlatitudes, there is an average cyclonic binary rotation up to ~2000 km with 98% statistical significance up to 1100 km.
- 4) The binary rotation rate decreases with the square of the separation distance, just as in the point vortex theory, up to 1400 km. But a pronounced unexpected peak was found near 1800 km. This peak is probably related to the rotation of secondary small-scale cyclones along the periphery of a primary large-core upper-level cyclone and is currently being explored.
- 5) The midlatitude binary rotation rate increases with the combined intensity in agreement with the point vortex theory, but no significant speed/intensity relation exists, in contrast with theory.
- 6) Contrary to the surface binary cyclones, the 500-hPa midlatitude binaries fit nicely the point vortex model based on the barotropic assumption.

A comparison between the barotropic theory and observations is summarized in Table 1. A better model

TABLE 1. Characteristics of the midlatitude surface binary surface cyclones: observations against main theoretical findings.

Characteristic	Findings	Comments
Cyclonic rotation	Up to a 2000-km separation	Observed values agree with theory
Rotation–separation relation	Agreement up to 1400 km	Unexplained peak near 1800 km
Rotation–intensity relation	Agreement	Cyclone intensity $\approx$ geopotential depth
Intensity–speed relation	No significant correlation	

for describing the binary surface cyclones should rely on atmospheric tracers, which have an association with surface cyclones such as the Ertel potential vorticity and potential temperature, which are the only invariant dynamic fields in adiabatic frictionless conditions (Egger 1989). In a companion study, we propose a three-dimensional model that applies the PV concept for explaining the binary cyclone behavior and clearly differentiates the upper level from the surface systems (Ziv and Alpert 1994).

*Acknowledgments.* We thank the German Israeli Bi-National Science Foundation (GIF) Grant I-138-120.8/89 for supporting this research. Mr. Y. Shay-El is acknowledged for the cyclone archive. Thanks to ECMWF for the data and to Prof. J. Egger and Dr. A. Tafferner for valuable comments. Special thanks go to the anonymous reviewers for helpful and very useful advice.

## APPENDIX A

### Relation Between Cyclone's Depth and its Induced Rotation

Equation (1) implies that the tangential speed  $V$  induced by a point vortex having intensity  $k$  as function of distance  $r$  is

$$V = \frac{k}{2\pi r}. \quad (\text{A1})$$

Assuming geostrophic balance,  $V$  can be expressed by the geopotential height field  $h$  according to

$$v_g = \frac{g}{f} \frac{\partial h}{\partial r}. \quad (\text{A2})$$

Equations (A1) and (A2) yield

$$\frac{k}{2\pi r} \approx \frac{g}{f} \frac{\partial h}{\partial r}. \quad (\text{A3})$$

Integrating (A3) from the margins of cyclone's core  $r_0$  to its outer radius  $R_0$  yields

$$\frac{kf}{2\pi g} (\ln R_0 - \ln r_0) \approx \Delta h. \quad (\text{A4})$$

Equation (A4) implies that the cyclone depth  $\Delta h$ , given in geopotential height terms, is proportional to its intensity, ignoring variations in  $R_0$  and  $f$ .

APPENDIX B

**Extraction of Binary System's Velocity from the Cyclones' Individual Velocities**

Lamb (1945) defines the location  $x_s$  of the centeroid (or rotation axis) of a binary system compound of cyclones 1 and 2 by

$$x_s = \frac{x_1 k_1 + x_2 k_2}{k_1 + k_2} \tag{B1}$$

Since in the absence of background flow this center is stationary, the velocity of the centeroid  $v_s$  is

$$v_s = \frac{v_1 k_1 + v_2 k_2}{k_1 + k_2} = \frac{v_1 M_1 + v_2 M_2}{M_1 + M_2} \tag{B2}$$

When subtracting  $v_s$  from the individual velocities of the binary constituent cyclones, the ratio  $V_2/V_1$  becomes identically equal to  $k_1/k_2$ , and the correlation becomes identically unity.

The use of an algebraic mean velocity for the system velocity yields  $V_2/V_1 = 1$  and, hence, no meaningful correlation is obtainable.

APPENDIX C

**Binary Interactions at 500-hPa Pressure Level**

The 500-hPa pressure level is frequently referred to as a nearly nondivergent and barotropic level. Though this work deals with surface cyclones, it is of interest to examine the binary interaction at 500 hPa. The following refers to 290 time sets chosen randomly from the study period and domain, containing 10 936 vortex pairs.

*a. Method of analysis*

The vortices were represented by local maxima in the relative vorticity, since closed circular isohypsies are not frequent in 500 hPa. The location and maximum values were extracted by a two-dimensional parabolic interpolation from the gridded data. The velocity of the  $i$  vortex at time set  $j$  with location  $\mathbf{x}_0$  was extracted according to the following steps. The first guess of displacement vector  $\Delta \mathbf{x}_0$  is

$$\Delta \mathbf{x}_0 = \Delta t \cdot \mathbf{V}_0, \tag{C1}$$

where  $\mathbf{V}_0$  is the 500-hPa wind vector at its initial location and  $\Delta t = 12$  h. The predicted location  $x_p$  for the next time set is, therefore,

$$\mathbf{x}_p = \mathbf{x}_0 + \Delta \mathbf{x}_0. \tag{C2}$$

The location  $x_j$  of the vortex found at the closest proximity to the predicted location at the next time set—if

$|x_j - x_p| < |\Delta x_0|$ —is referred to as the next-step location of vortex  $i$ . Hence, the instantaneous velocity  $V_0$  of vortex  $i$  at time set  $j$  is

$$\mathbf{V}_0 = (\mathbf{x}_j - \mathbf{x}_0) / \Delta t. \tag{C3}$$

A subjective examination of 30 tracks of vortices has confirmed this procedure. The rotation factor was then extracted in the same method presented in section 4.

*b. Results*

For barotropic conditions, the 500-hPa average wind may be considered as the background flow. At lower latitudes the positive vorticity within the cyclonic vortices is of the same order of magnitude as for the background flow, and is about  $-2 \times 10^{-6} \text{ s}^{-1}$  between  $10^\circ$  and  $20^\circ \text{N}$  (figure not shown). The average vorticity at  $30^\circ$ – $60^\circ \text{N}$  for the study period is  $\approx 0.5 \times 10^{-6}$ , which is one to two orders of magnitude smaller than that found within the cyclonic vortices. The following refers to 1023 isolated (section 6) pairs in the  $30^\circ$ – $60^\circ \text{N}$  latitudinal domain.

The average rotation factor (Fig. C1, solid line) is positive for all separations. The positive values at separations larger than the Rossby radius of deformation may be explained by the effect of the background vorticity (section 8). Indeed, the bias of 0.02 in the rotation factor is consistent with the average background

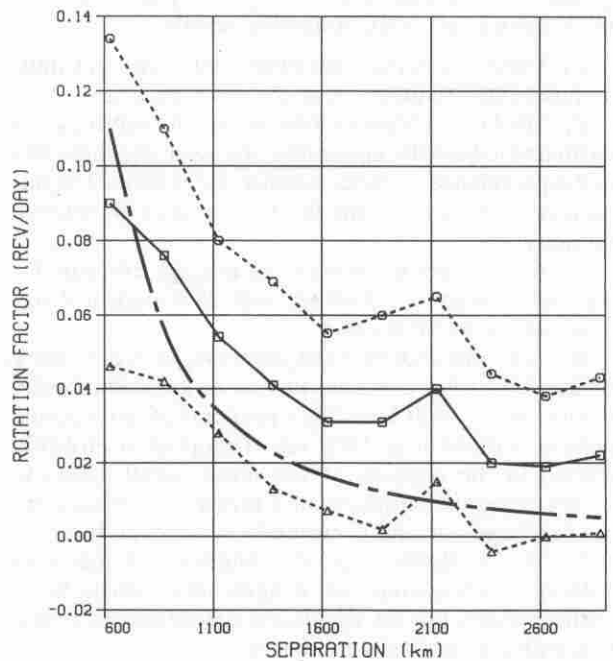


FIG. C1. Variation of average isolated 500-hPa vortex pairs rotation factor in units of rotations per day as a function of their separation distance (solid) for the same area and 290 time sets out of the period as in Fig. 3. Dashed lines indicate the limits of 98% confidence interval. The semidashed line shows the theoretical relationship. This figure corresponds to Fig. 8 for the surface cyclones.



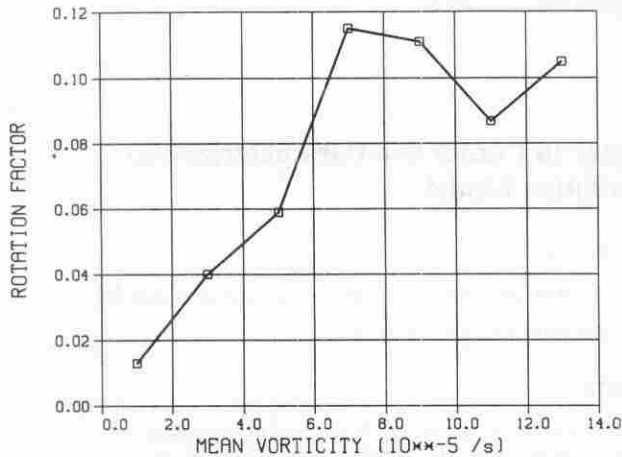


FIG. C2. Variation of rotation factor with the mean intensity for the sample as in Fig. C1 and for separation distances of 500–2500 km. The intensity is expressed by the vorticity at the vortices centers. This figure corresponds to Fig. 9a for the surface cyclones.

vorticity. The rotation/separation relationship agrees well with theory (Fig. C1, semidashed), except for the minor peak near the 2100-km separation. The rotation/intensity relation (Fig. C2) is also in agreement with the theoretical linear relationship. The correlation between the rotation speeds and intensities were examined for various subsamples of vortices rotating cyclonically with the separation of 500–2500 km. The intensities were represented by the vorticity maxima and only the meridional speeds were accounted to eliminate the shear contribution. The correlations were, nevertheless, insignificant (0.1) when all the reduced sample was included, but increased when only intense pairs were considered. For vortices with maximum vorticity exceeding  $7 \times 10^{-5} \text{ s}^{-1}$  (80 cases) it increased to 0.36.

In summary, the 500-hPa pressure level results resemble, as expected, the binary interaction barotropic model much better than the surface results, though some discrepancies still exist, due, among others, to an inevitable noise, which characterizes the real atmosphere.

#### REFERENCES

- Alpert, P., and B. Ziv, 1989: The Sharav Cyclone—Observations and some theoretical considerations. *J. Geophys. Res.*, **94**, 18 495–18 514.
- , B. U. Neeman, and Y. Shay-El, 1990a: Climatological analysis of Mediterranean cyclones using ECMWF data. *Tellus*, **42A**, 65–77.
- , —, and —, 1990b: Intermontly variability of cyclone tracks in the Mediterranean. *J. Climate*, **3**, 1474–1478.
- Aref, H., 1983: Vortex motion. *Ann. Rev. Fluid Mech.*, **11**, 95–122.
- Batchelor, G. K., 1980: *An Introduction to Fluid Dynamics*. 5th ed., Cambridge University Press, 615 pp.
- Bengtsson, L., M. Kanamitsu, P. Kallberg, and S. Uppala, 1982: FGGE 4—dimensional data assimilation at ECMWF. *Bull. Amer. Meteor. Soc.*, **63**, 29–43.
- Brand, S., 1970: Interaction of binary tropical cyclones of the western North Pacific Ocean. *J. Appl. Meteor.*, **9**, 433–441.
- Chang, S. W., 1983: A numerical study of the interaction between two tropical cyclones. *Mon. Wea. Rev.*, **111**, 1806–1817.
- DeMaria, M., and J. C. L. Chan, 1984: Comments on "A numerical study of the interaction between two tropical cyclones." *Mon. Wea. Rev.*, **112**, 1643–1946.
- Dong, K., and C. J. Neuman, 1983: On the relative motion of binary tropical cyclones. *Mon. Wea. Rev.*, **111**, 945–953.
- Egger, J., 1989: A note on the complete sets of material conservation laws. *J. Fluid Mech.*, **204**, 543–548.
- Falkovich, A. I., A. P. Khain, and I. Ginis, 1995: Motion and evolution of binary tropical cyclones in a coupled atmosphere–ocean numerical model. *Mon. Wea. Rev.*, **123**, in press.
- Fujiwhara, S., 1923: On the growth and decay of vertical systems. *Quart. J. Roy. Meteor. Soc.*, **49**, 75–104.
- , 1931: Short note on the behavior of two vortices. *Proc. Physico-Mathematical Soc.*, Vol. 13, 3d ed., Japan, 106–110.
- Gill, A. E., 1982: *Atmosphere–Ocean Dynamics*. Academic Press, 662 pp.
- Haseler, J., and G. Sakellarides, 1986: Description of the ECMWF model post processing system. Tech. Memo No. 121, ECMWF.
- Haurwitz, B., 1951: The motion of binary cyclones. *Arch. Meteor. Geophys. Bioklim.*, **B4**, 73–86.
- Holland, G. J., and M. Lander, 1993: The meandering nature of tropical cyclone tracks. *J. Atmos. Sci.*, **50**, 1254–1266.
- Hollingworth, A., D. B. Shaw, P. Lonnberg, L. Illari, K. Arpe, and A. J. Simmons, 1986: Monitoring of observations and analysis quality by a data assimilation system. *Mon. Wea. Rev.*, **114**, 861–879.
- Holton, J. R., 1992: *An Introduction to Dynamic Meteorology*. 3d ed., Academic Press, 511 pp.
- Hoover, E. W., 1961: The motion of hurricane pairs. *Mon. Wea. Rev.*, **89**, 251–255.
- Hopfinger, E. J., and G. J. F. van Heijst, 1993: Vortices in rotating fluids. *Ann. Rev. Fluid Mech.*, **25**, 241–289.
- James, R. W., 1950: On the theory of large-scale vortex rotation in the atmosphere. *Quart. J. Roy. Meteor. Soc.*, **76**, 255–276.
- Lamb, H., 1945: *Hydrodynamics*. 6th ed., Dover Publications, 738 pp.
- Mattocks, C., and R. Bleck, 1986: Jet streak dynamics and geostrophic processes during the initial stages of lee cyclogenesis. *Mon. Wea. Rev.*, **114**, 2033–2056.
- Neeman, B. U., and P. Alpert, 1990: Visualizing atmospheric fields on a personal computer: Application to potential vorticity analysis. *Bull. Amer. Meteor. Soc.*, **71**, 154–160.
- Shay-El, Y., and P. Alpert, 1991: A diagnostic study of winter diabatic heating in the Mediterranean in relation with cyclones. *Quart. J. Roy. Meteor. Soc.*, **17**, 715–747.
- Stein, U., and P. Alpert, 1993: Factor separation in numerical simulation. *J. Atmos. Sci.*, **50**, 2107–2115.
- Tafferer, A., 1990: Lee cyclogenesis resulting from the combined outbreak of cold air and PV against the Alps. *Meteor. Atmos. Physics*, **43**, 31–47.
- Ziv, B., and P. Alpert, 1994: A potential vorticity conceptual model to the binary cyclone. *The Life Cycle of Extratropical Cyclones*, S. Gronås and M. A. Shapiro, Eds., Vol. II, Amer. Meteor. Soc., 370–375.